

## **LABORATORY TESTING AND MODELING THE INTERFACIAL TRANSITION ZONE OF SLAG-CONCRETE**

Han Ay Lie<sup>1</sup>, Nuroji<sup>1</sup>

*Diterima 04 Mei 2009*

### **ABSTRACT**

*The transition zone at the aggregate surface has a distinctive formation, in terms of its mechanical as well as its physical properties. This layer is recognized as the ITZ (Interfacial Transition Zone) and considered the “weak link”, since micro cracks are commonly initiated in this area. The properties of this ITZ are yet to be investigated. SEM (Scanning Electron Microscope) images only provide qualitative information such as formation, type and relative amount of crystals. Therefore, other means are required to represent a better understanding to the behavior of the ITZ. The mechanical and physical properties of the ITZ are highly influenced by the differentiation in porosity and strength. A mathematical or FEM (Finite Element Model) can be used to bridge this lack of information. This paper deals with the the modeling approach of ITZ as well as the concept of laboratory testing for validation of the model.*

**Keywords:** *labour group composition, SNI 2002, field labour’s productivity, middle-class housing.*

### **ABSTRAK**

*Daerah peralihan antara agregat dan mortar memiliki susunan struktur dan sifat mekanis yang berbeda dengan mortar yang berjauhan dari agregate. Daerah ini dikenal sebagai ITZ (Interfacial Transition Zone) dan diketahui sebagai daerah yang “lemah” karena retak mikro biasanya diawali di ITZ ini. Perilaku mekanis ITZ sangat sulit ditentukan secara tepat, pengamatan menggunakan SEM (Scanning Electron Microscope) hanya dapat memberikan gambaran secara kualitatif, berupa perilaku bentuk, susunan dan jumlah kristal sehingga perlu adanya pendekatan lain yang dapat memberikan nilai kuantitatif terhadap perilaku ITZ. Pengamatan terhadap sifat mekanis dan fisis ITZ terhadap mortar menunjukkan perbedaan kadar pori dan kekuatan. Untuk menggambarkan konfigurasi pori dan kekuatan ITZ dapat digunakan model, baik model matematis atau FEM (Finite Element Model) yang divalidasi dengan hasil pengujian laboratorium. Tulisan ini membahas konsep permodelan ITZ serta metoda validasi di laboratorium.*

**Kata kunci:** *model, interfacial transition zone, mortar, aggregate, kekakuan*

---

<sup>1</sup> Jurusan Teknik Sipil Fakultas Teknik Universitas Diponegoro  
Jl. Prof. Soedarto SH, Tembalang Semarang, 50275  
Email : aylichan@indosat.net.id; nrji@sipil.ft.undip.ac.id

## INTRODUCTION

Modeling takes an important role in describing the behavior of materials or structural elements. A model is especially important in cases where fullscale or laboratory scale experiments are difficult to achieve, are extremely expensive, having a high safety risk or technically time consuming. Further, modeling can function as a validating tool to a laboratory experiment or used as comparison to other typical models.

Basically, a model is a method of visualization physical interactions of an element. A model has the advantage that theoretically no limitations exist to the number of specimens being tested, while human errors can be minimized.

The main challenges in constructing a model are: the lack of actual structural behavior's knowledge; theoretical understanding limitations; elements' behavior predictions and program inadequacy.

The discrediting techniques will highly influence the resulting data. Automatic mesh generators will enable a programmer to obtain a smooth stress behavior. To construct a good model many aspect has to be defined such as: loading conditions; static and dynamic responses; boundary conditions; buckling; isotropic and orthotropic behavior; the presence of plastic flow and numerous non-linearity issues that has to be considered.

Concrete is a three phase material. The properties of aggregates, mortar and concrete are widely known. The most influential properties are the Modulus of Elasticity ( $E$ ), Poisson's ratio ( $\nu$ ), tensile strength ( $f_t$ ) and compression strength ( $f_c$ ).

Since concrete is a nonlinear inelastic material, the modulus of elasticity for concrete and mortar is represented by its *initial tangent modulus* (Mehta and Monteiro 1993; Mindess,

Young and Darwin, 2003; Neville, 2003). Since the initial tangent modulus only represents the material at very low stress levels, the *secant modulus*, being the slope between the origin and the point on the stress-strain curve, gives a better behavior representation (Figure 1.).

ASTM C469 chapter 14 describes the *chord modulus* as the slope of a line that connects two points on the curve. The lower point is set at a strain of 0.00005 corresponding to the initial tangent modulus.

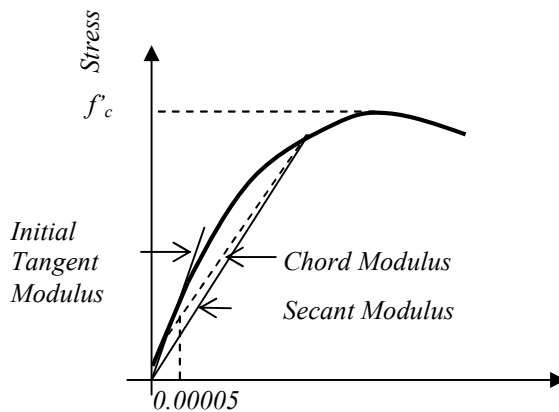


Figure 1. Initial, tangent and secant stiffness iteration

Mortar has an approximately similar stress-strain relationship to concrete. The modulus of elasticity methodology for concrete should therefore be applicable to mortar. However, Neville (1997, 2003); Scrivener et. al. (2004), concluded that the stress-strain relationship of cement paste follows a linear pattern. Concrete and mortar nonlinearity is thus an integrated result of aggregate, ITZ and cement behavior. For aggregates, the stress-strain curves are linear up till failure (Mehta and Monteiro, 1993; Han and Purwanto, 2009), and the initial tangent modulus will represent the material stiffness accurately. 7

Mehta and Monteiro (1993) concluded that the tensile strain rather than the tensile strength determines the failure in uniaxial compression.

Typical stress-strain curves were summarized and presented in Figure 2. Since the ITZ is considered as shell surrounding the aggregates, and the majority of tension fracture occurs in this area, it could be well assumed that this relationship represents the ITZ behavior in tension, to a certain degree.

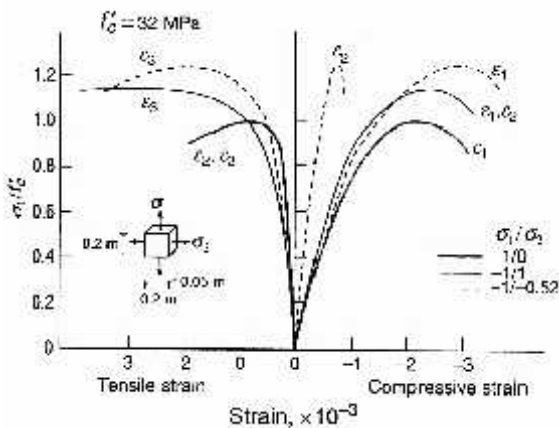


Figure 2. Stress-strain behavior of concrete in tension (Mehta et. al. 1993)

### THE INTERFACE TRANSITION ZONE, LITERATURE REVIEW

The ITZ differs noticeably from the mortar mass. Various models have been proposed to illustrate the zone, adjacent to the aggregate surface. Among these are; *Barnes - Diamond - Dolch (1978)*; *Langton (1980)*; *Ollivier - Grandet (1982)*; *Zimbelmann (1985)*; *Mehta - Monteiro (1993)*; *Bentur - Odler (1996)*; *De Rooij - Bijen - Frens (1998)*. The majority was based on SEM and X-ray diffraction observations, while various aggregate types were used, ranging from natural stones to glass and metal aggregates. The most distinctive models are listed (Figure 3).

The ITZ is known as the “weak link” in concrete (*Monteiro et. al., 1985*; *Mehta and Monteiro, 1993*; *Scrivener and Pratt, 1996*;

*Mindess et. al., 2003*; *Besari, 2007*). The researches on ITZ chronologically, are as follows:

*Barnes et. al. (1979)* conducted experiments using *glass aggregates* and concluded that the micro morphological features of their ITZ are similar to the standard aggregates.

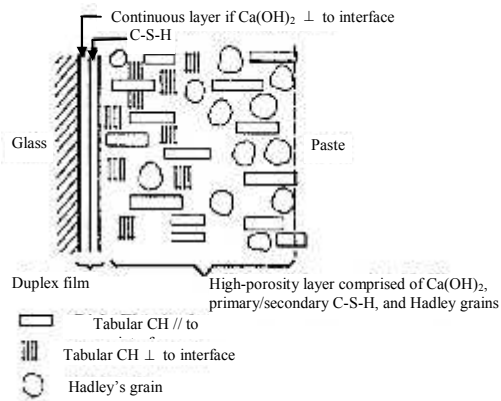
*Monteiro et. al. (1985)* recognized the ITZ as the “weak link” due to higher porosity; formation of large crystals of the hydration products and the calcium hydroxide crystals deposition with a preferential orientation. Monteiro also stated that the ITZ thickness depends on the size and shape of aggregates.

*Pope and Jennings (1992)* stated that the porosity and amount of anhydrous cement particles in the ITZ depends upon the water at the aggregate surface, during mixing. Further, concluding that mixing methods can influence the ITZ behavior significantly.

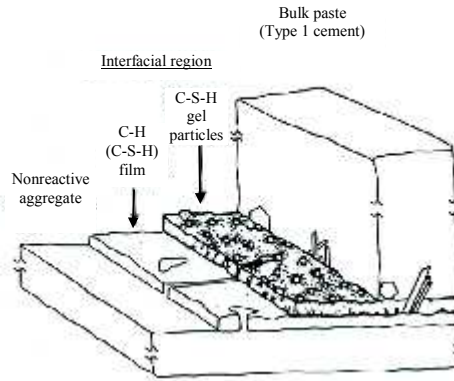
*Breton et. al. (1993)* evaluated the various models developed to describe the ITZ and found that a single model representing the only mortar paste, is insufficient in describing the ITZ behavior.

*Bonen (1994)* used the SEM *back scattered* method to observe the ITZ and found that it has a thickness of 2 to 8  $\mu\text{m}$ , and is dominated by CH deposits and large pores. The region is therefore vulnerable to solution ingress and chemical attacks. *Bonen* disagreed that the crystal formation was influenced by the water film around the aggregates, as was stated by *Zimbelman (1987)* and *Pope (1992)*.

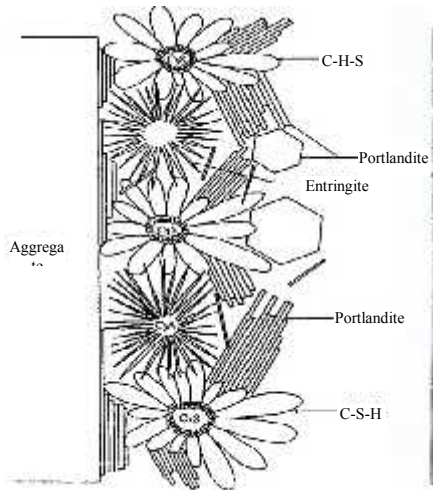
*Diamond and Mindess (1991)* and *Diamond and Huang (2001)* performed extensive SEM examinations and concluded that the ITZ basically did not differ significantly enough from the mortar, to affect the mechanical properties of concrete. *Diamond* used well graded, well mixed concrete compositions.



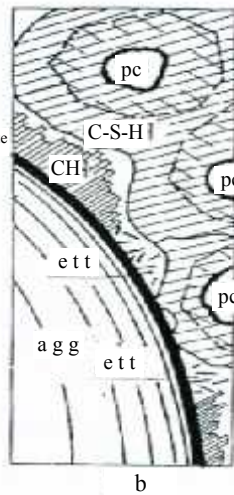
a. Diamond's Model, adapted by Brenton (1993)



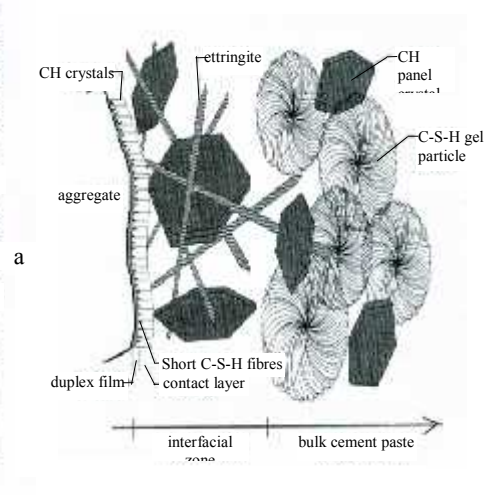
b. Langton's Model, adapted by Mindess (2003).



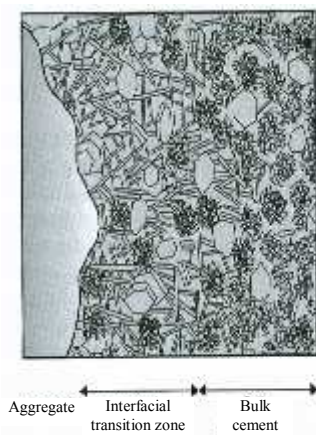
c. Ollivier's Model, adapted by Brenton (1993)



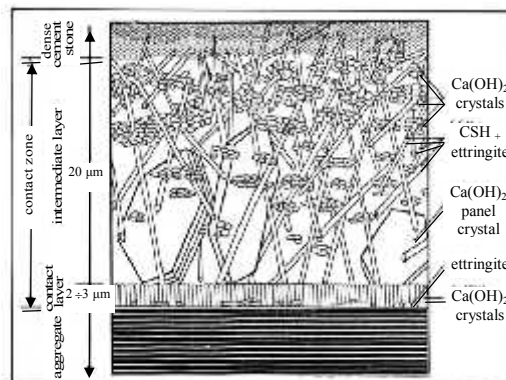
d. Bentur's Model (1996)



e. De Rooij's Model (1998)



f. Monteiro's Model (1993)



g. Zimbelmann's Model (1985)

Figure 3. Various Illustration of the ITZ

Rao and Prasad (2002) conducted tests to obtain tensile and shear strength of the ITZ. It was shown that the tensile capacity is significantly lower than the mortar. Values of one third to one twentieth were reported. The ITZ is according to Rao, a result of higher water-cement-ratio at the aggregate surface's and the wall-effect. Further he indicated that the shear strength of ITZ depends on surface roughness and type of mortar.

Harutyunyan et. al. (2003) used SEM readings to explain the amount of planar defect, cracks and possible stacking faults within the ITZ. In the research, reading was done with the X-ray diffractometer (a technique of reading the bending and spreading of waves as they pass round the edge of an obstacle). Marble, glass and quartz aggregates were chosen to simulate aggregates. It was found that the ITZ has a highly complicated strain and strain dispersion, and most of the CH crystals are subjected to compression strain.

Elsharief et. al (2003) did tests on the influence of aggregate type and gradation to the properties of concrete, and found that an increase in aggregate size would increase the porosity and thickness of the ITZ. His study was conducted by observing the absorption and resistance to sulfate solution attacks.

Scrivener et. al. (1996; 2004) portrayed the ITZ as cement paste that is perturbed by the presence of aggregates, causing an increase in porosity and predominance of smaller cement particles. Scrivener used the SEM back-scattering techniques and concluded that the ITZ was influenced by the "wall" effect (Figure 4) where the formation of a grain cross a flat solid object, is disturbed. Further, it was found that the ITZ has a thickness of 15 to 20  $\mu\text{m}$  independent of the water-cement-ratio, and that the ITZ leads to increase of ductility.

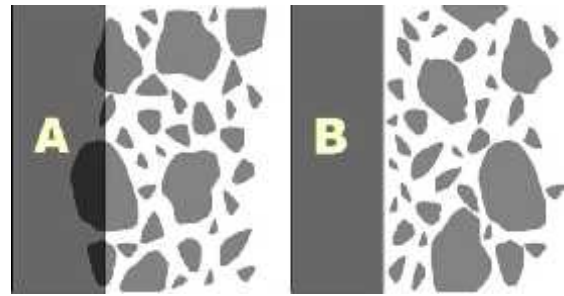


Figure 4. Illustration of the "wall" effect on the ITZ (Scrivener, 2004)

Akçaoğlu et. al. (2004) performed uni-axial compression tests on single spherical steel aggregates of different sizes, and discovered that the ITZ becomes critical for larger aggregates. Compression stresses were also found to be sensitive to the smooth surface, and the large difference in modulus of elasticity between mortar and steel. They concluded that the ITZ has little effect to the compression strength, but is the determining factor when in tension. High water-cement-ratios have a pronounced effect up to the onset of crack propagation, but for rapid cracks, low w/c mixtures were more influential.

Besari (2007) declared that the formation of ITZ is an effect of water accumulation around the aggregates called *bleeding*. When evaporated during the hardening process, this leaves a micro gap filled with weak CH crystals.

Head et. al. (2008) developed a new technique to elucidate the ITZ quantitatively, with 3D laser scanning readings. The capillary porosity and anhydrous cement particles were plotted against their distance to the aggregate surface. Head established that the porosity is 45-55% at the interface directly adjacent to the aggregate, and reduces to 15% at a distance of 20-30  $\mu\text{m}$ . The anhydrous cement particles were found to be zero at the interface, but rises with distance for the aggregates due to the particle packing.

The ITZ is unquestionably dissimilar to the mortar further away from the aggregate's surface. This zone is a thin shell, having a thickness dependent on *surface roughness; aggregate type and gradation; moisture conditions and w/c factor; the presence of water film surrounding the aggregate and the effect of bleeding*. Visual observations indicate this shell's thickness as to be 15 to 50  $\mu\text{m}$ . Porosity in this area is higher, which can be explained by the *wall effect* or *micro gap* surrounding the aggregates. Higher porosities lead to a weaker zone, both in tension and shear. However, direct testing of mechanical properties has not been conclusive.

The SEM or X-ray observations are qualitative in nature, the ITZ mechanical properties can't be concluded based on these readings alone. Modeling techniques provide more actual outcomes, in explaining the ITZ property.

### MODELING OF THE ITZ

Concrete consists of aggregates, embedded in a mortar matrix. Whereas the aggregate has a linear stress-strain behavior up till its ultimate strength, the mortar exhibits a highly non-linear behavior. The ultimate strength of the *Pudak Payung* as well as slag aggregates is noticeably higher than that of mortar.

Also, based on preliminary test results it is shown that the stiffness of both materials differs significantly. When subjected to loading, this will lead to stress disparity in both the mortar and aggregates. The overall behavior becomes a complex issue, even when assuming a perfect bond between aggregate and mortar.

The relatively high difference in stiffness and compression strength between aggregates and mortar, will accentuate stress concentration. Since the ITZ is recognized as the weak link in concrete, these stress concentrations will in turn, lead to micro crack initiation in this area (*Cody et. al., 2001; Vervuurt, 1998; Diamond*

*and Mindess, 1991; Barnes et. al., 1997*), further developing in mortar crack propagations.

The stiffness as well as the stress-strain relationship of the ITZ therefore becomes very important to explain the overall behavior of concrete. *Godier (1933); Bremner and Holm, (1986)* and *Neville (2003)* illustrated these stress concentrations around spherical inclusions subjected to a unit applied infinite stress (Figure 5).

Based on *Bremner and Holm's* model, a typical 2 D specimen was constructed and analyzed by the SAP 2000 program. The model is a 50x50 mm mortar specimen with a single inclusion 20 mm in diameter. A unit displacement is applied on the upper and bottom surface, creating an uniaxial loading condition. (Figure 6).

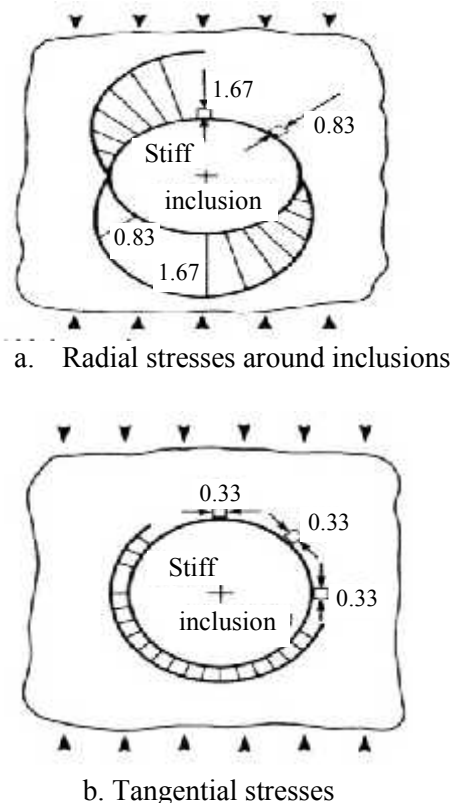


Figure 5. Stress concentrations around inclusions (Benner, 1986)

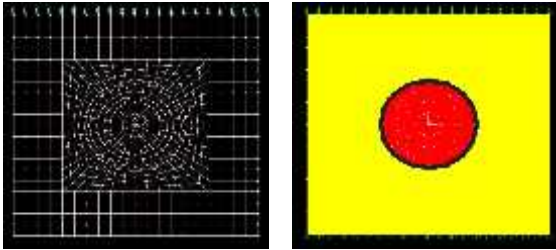


Figure 6. The 2D SAP 2000 model subjected to a unit compression force.

Whereas the ITZ thickness does not accurately model its real 50  $\mu\text{m}$  value, a sufficiently large *length-to-thickness* ratio will give a good illustration to the stress distribution in the specimen. This approach will further prevent *ill conditions* and the present of *poor elements* in the SAP model.

A perfect bond is assumed and three different model-specimens are constructed. The first having an inclusion with the same properties as the mortar matrix; while the second model's inclusion has a significantly higher stiffness than the mortar. The third specimen has a thin layer surrounding the inclusion, imitating the ITZ by setting a very low stiffness value. The properties are listed in Table 1.

The SAP 2000 program will generate the nodal stresses as to be the principal stresses (maximum and minimum). The maximum stress is the extreme principal tensile stress and the minimum stress is the principal compression stress, as described in *Möhr's circle* (Figure 7).

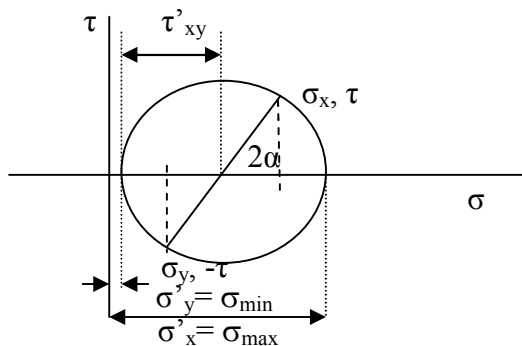
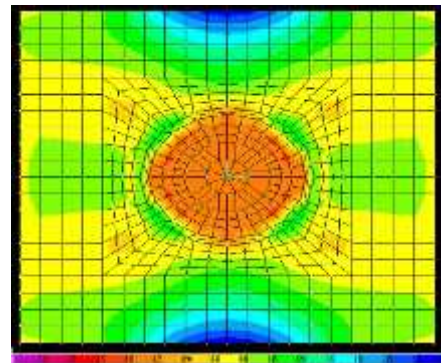
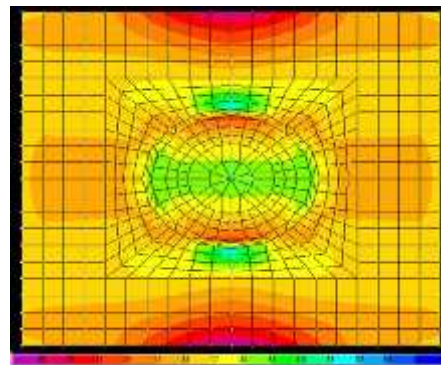


Figure 7. Möhr's circle representing maximum and minimum nodal stresses.

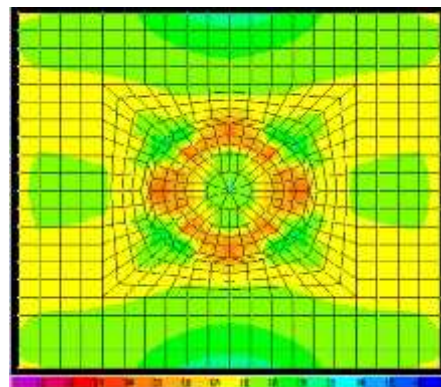
Figures 8 and 9 demonstrate the elastic models' stress distribution of a specimen with a single inclusion subjected to a uniform displacement of one unit at the top fibers. While the principal stresses' trajectories are represented in Figure 10 and 11.



a. Mortar sample



b. Embedded aggregate, no ITZ



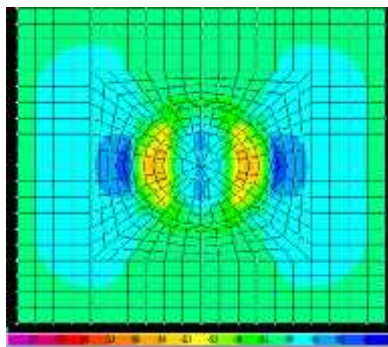
c. Embedded aggregate with ITZ

Figure 8. Principal Tensile Nodal Stresses

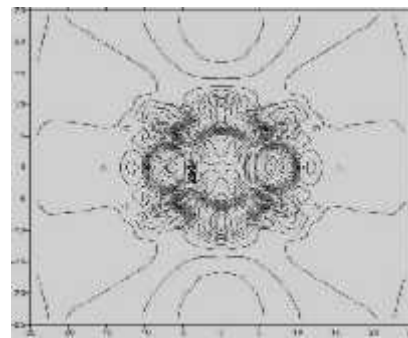
Table 1. Mortar, aggregate and ITZ properties

Properties	Pudak Payung aggregates	Mortar	ITZ
Mass density $\gamma$ (grams/cm <sup>3</sup> )	0.28		-
Modulus of elasticity E (Gpa)	57.58	26.22	1.00
Poisson's ratio $\mu$	0.35	0.23	0.30
Compression strength $f'_c$ (Mpa)	79.6	52.4	-

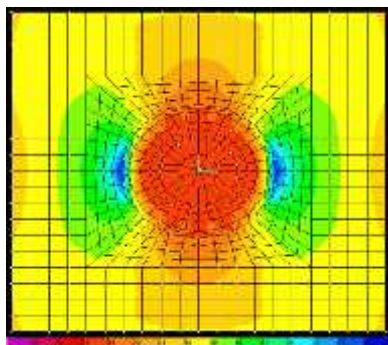
Source : Han Aylie and Purwanto, 2009



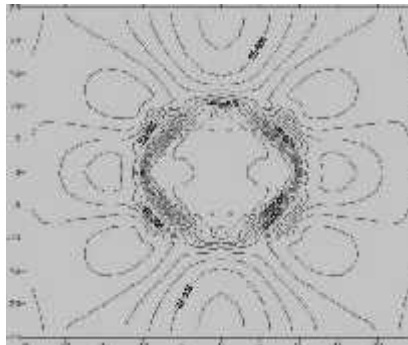
a. Mortar sample



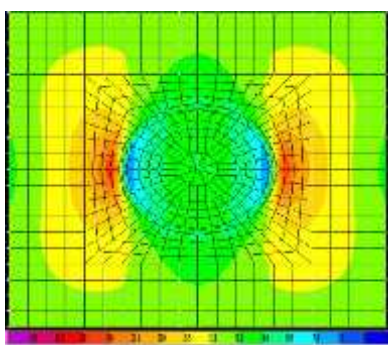
a. Mortar sample



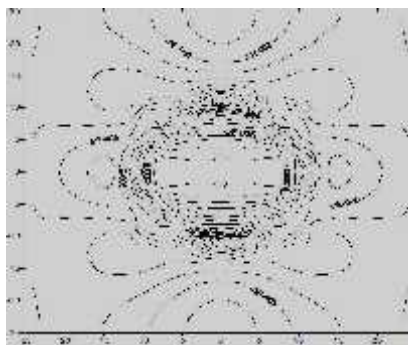
b. Embedded aggregate, no ITZ



b. Embedded aggregate, no ITZ



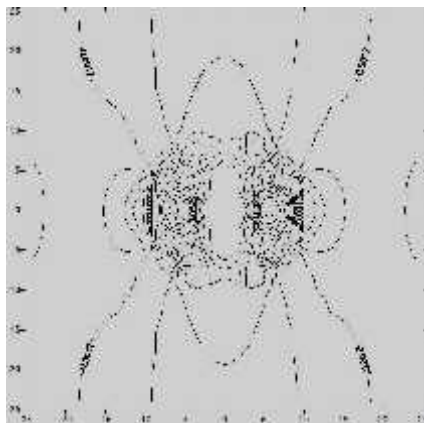
c. Embedded aggregate with ITZ



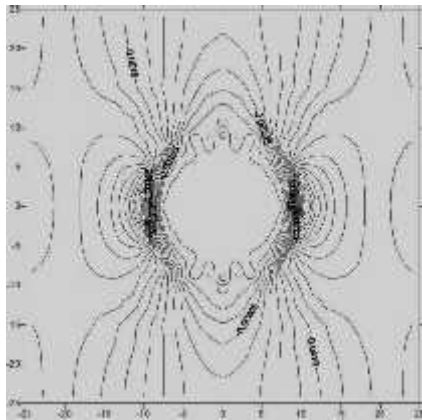
c. Embedded aggregate with ITZ

Figure 9. Principal compression nodal stresses

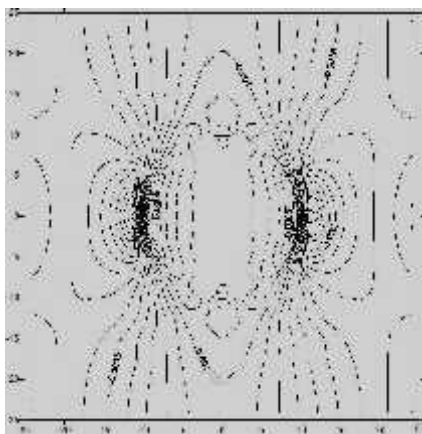
Figure 10. Tensile stress trajectory



a. Mortar sample



b. Embedded aggregate, no ITZ



c. Embedded aggregate with ITZ

Figure 11. Compression stress trajectory

Figures 8 and 9 show the shifting in principal stresses due to stiffness differences. The all-

mortar specimen has stress levels varying from 0.0002 to  $-0.0027$ .

For the sample with an embedded aggregate, pronounced stress disparities were resulted. The principal tensile and compression stress levels were ranging from 0.0001 to  $-0.0022$ .

Next, the ITZ represented by a layer with a very small *thickness-to-length* ratio surrounding the solid, was added. This superficial ITZ has a stiffness ratio 25 times *lower* than the mortar. Large stress disparities were now perceived. Principal stresses were ranging from 0.0004 to  $-0.0025$ .

Stress evaluation showed that the ITZ will contribute significantly to the stress disparity. Not only does the ITZ influence this stress pattern, it also affects the concrete failure mode, shifting it from compression to tension.

Research work has proven that the ITZ does not provide a perfect bond between aggregates and mortar (*Harutyunyan et. al., 2003; Neville, 1997; Roy et. al., 1993*). Assuming a perfect bond thus can lead to inappropriate conclusions and deviations from real concrete behavior.

Since the ITZ has a thickness of only  $50 \mu\text{m}$ , data obtained from laboratory testing are not easy to achieve. Scanning Electron Microscopic (SEM) images on the other hand, can only present qualitative, rather than quantitative data. Therefore a FEM model, validated by laboratory tests will be used to obtain the properties of the ITZ.

### Shear and Normal Stiffness

Research material concerning the ITZ' shear and normal stiffness's is limited. *Harutyunyan et. al. (2003)* stated that as a result of CH crystal formations, large shear strains occur in this area, leading to deformation and micro cracking initiation. *Bentur and Alexander (2000)* underlined that models require accurate

information about interface tensile and shear strength. Šmilauer and Bittnar (2006) concluded that based on his numerical model, the ITZ shear stiffness has very little contribution to the ITZ strength.

The Hashin-Shtrikman's model was elaborated by Nilsen and Monteiro was evaluated, but no exact values were obtained. Rao and Prasad (2002) conducted experiments to evaluate the aggregate roughness effect to the ITZ shear capacity. Further, their research proved that the surface-inclination-to-load influences the shear strength positively.

The FEM model of Kwan et. al. (1999) gave a good approximation to the interface's shear and normal stiffness. However, the results were not validated with real tested specimens. Mitsui et. al. (1994) represented the interface's shear capacity by describing the relationship of pull-out load to slip displacement. Then, the mechanical parameters of the ITZ can be expressed in terms of the initial stiffness, shear bond strength and interfacial fracture energy.

The model of Hashim and Monteiro (2002) predicted that the Young's modulus of the ITZ is close to 50% that of the bulk cement paste.

Nagai et. al. (2004, 2005) calculated the ITZ stiffness as a function of the concrete elastic modulus ( $E_{element}$ ) and Poisson's ratio ( $\nu_{element}$ ):

$$k_n = \frac{E_{element}}{1 - \nu_{element}^2} \dots\dots\dots (1)$$

$$k_s = \frac{E_{element}}{1 + \nu_{element}} \dots\dots\dots (2)$$

Where  $E_{element}$  and  $\nu_{element}$  are the corrected elastic modulus and Poisson's ratio of components at meso-scale.

$$\nu_{element} = 20v^3 - 13,8v^2 + 3,8v(0 \leq v \leq 0,3) \dots\dots (3)$$

$$E_{element} = (-8\nu_{element}^3 + 12\nu_{element}^2 - 0,2\nu_{element})E \dots\dots (4)$$

Nie and Basaran (2005) developed a CSA (Composite Sphere Assemblage). The interface properties are the bulk modulus  $k$  and the shear modulus  $\nu$ . A numerical formulation was used, to calculate these properties based on the elastic modulus deviation by Hashin and Monteiro (2002) and the effective shear modulus by Christensen and Lo (1979). All interface properties were expressed as a function of the interface parameter  $q$ :

$$q = \frac{E_{filler}}{E_{matrik}} \dots\dots\dots (5)$$

Where:

$E_{filler}$  = Elastic modulus of inclusion

$E_{matrik}$  = Elastic modulus of mortar

Tensile stress rather than stiffness was reported by Sideridis et. al. (2007). The model was constructed of controversial square-in-square and cube-in-cube models, and gave a good estimate to the laboratory specimen behavior.

In lieu of limiting the  $k_n$  and  $k_v$  boundaries, the following experimental tests have to be conducted, and the load-deformation relationship assuming linearity, defined.

$$\begin{bmatrix} P_n \\ P_v \end{bmatrix} = \begin{bmatrix} k_n & 0 \\ 0 & k_v \end{bmatrix} \begin{bmatrix} dy \\ dx \end{bmatrix} \dots\dots\dots (6)$$

The load-deformation correlation can be presented graphically (Figure 12). Since deformations are small, a linear function is considered sufficiently accurate in predicting the  $k$  values.

Table 2. SAP analysis stress level evaluation

Specifications	Mortar	Embedded aggregate	Embedded aggregate and ITZ
Principal Tensile Stress	0.0002	0.0001	0.0004
Principal Compression stress	-0.0027	-0.0022	-0.0025
Tension/Comp stress Ratio	0.07	0.045	0.16
Failure mode	Compression	Compression	Tension

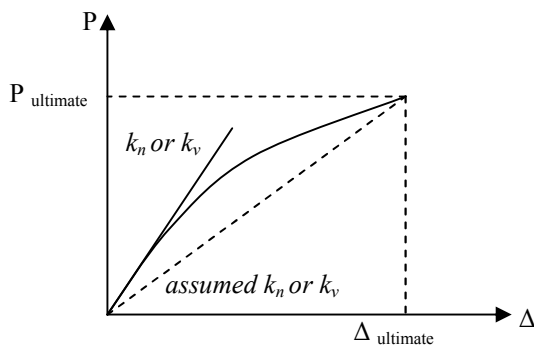


Figure 12. Load-deformation Relationship for  $k_n$

### Experimental Set-up

#### Normal stiffness $k_n$

To obtain the interface' normal stiffness, an experimental model has to be constructed, enabling only the normal ITZ response. The *Dyna Proceq haftprufer pull-off tester Z16* (Figure 13a) having a pull-out capacity of 16 kN will be used. A circular 2" diameter aggregate will be placed on top of the mortar matrix (Figure 13c). To minimize bleeding, w/c is reduced using *super-plasticizer*. Immediately after cement setting time, the cast is turned 180°, and the specimen kept moist for 28 days.

The aggregate is pulled-off by the tester, the maximum load measured, and the strain deformation recorded using LVDT's. To incorporate the effect of surface roughness, two aggregate types will be tested; the actual and the disturbed aggregate. The disturbed

surface is a result of grinding (figure 13b). The roughness ratio  $m$  can be calculated as:

$$m = \frac{k_{disturbed}}{k_{undisturbed}} \dots\dots\dots (7)$$

The “ $m$ ” ratio will further be incorporated into the FEM model.

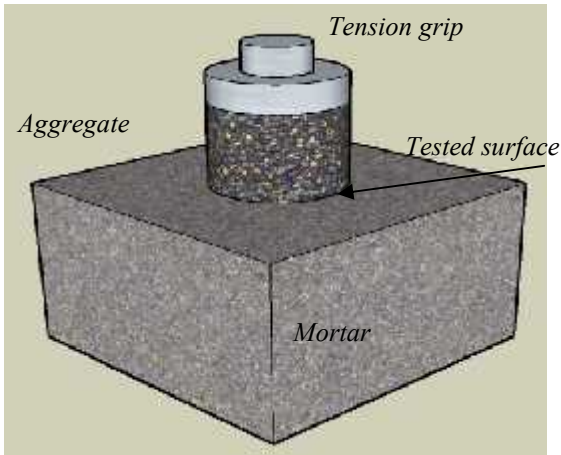


a. Dyna Pull-off Tester



b. Disturbed and undisturbed surface

Figure 13. The proceq-dyna pull-off tester and aggregate assemblage



c. Experimental Set-up

Figure 13. The proceq-dyna pull-off tester and aggregate assemblage (continuation)

**Shear stiffness  $k_v$**

The shear stiffness can be acquired by the following test (Figure 14). To ensure undisturbed or disturbed surfaces, the specimen will be manufactured using *Hiltibonding* agents (Figure 15) and taken from the natural stone (Figure 16).

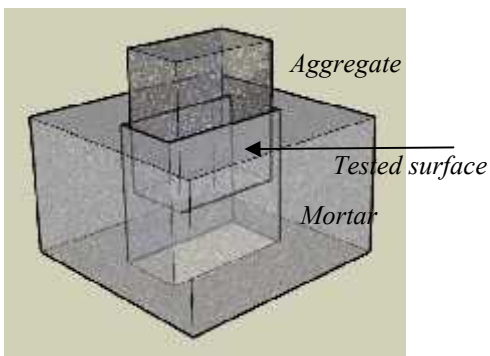


Figure 14. Shear stiffness experiment.

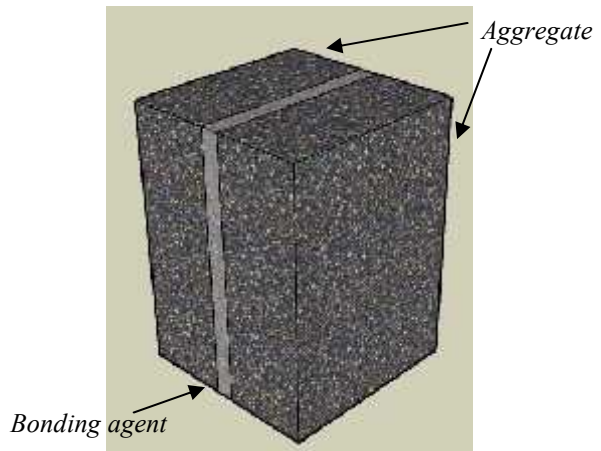


Figure 15. Shear stiffness specimen.

The aggregate undergoes an axial compression force and the stress will be calculated, the area being the contact field between aggregate and mortar. The deformation is recorded with LVDTs. The outer gap is created using a *styrofoam* cast, so that the aggregate will have two contact areas with the mortar.

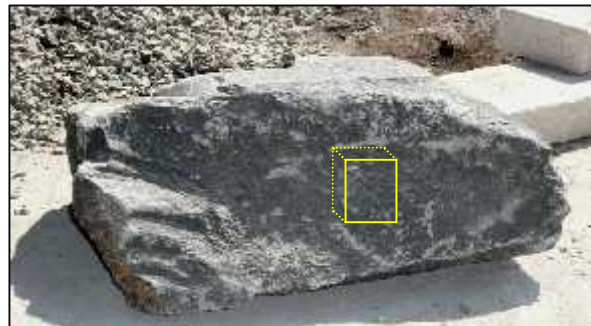


Figure 16. Specimen assemblage from natural stones

To incorporate area effect, a graphical presentation of the stress to area relationship will be constructed. This relationship will demonstrate the accuracy of  $k_v$  and  $k_n$  obtained by the proposed testing methods when used in the model (Figure 17). The function can further be used to correct the laboratory  $k_v$  and  $k_n$  of the

actual ITZ area within the model (*Grassi and Zdené., 2009*).

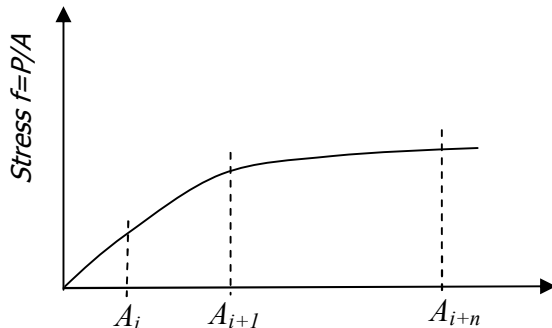


Figure 17. Stress area relationship for FEM model correction factors

The influence of bleeding to the ITZ normal and shear stiffness will be accommodated by casting the aggregates on top (simulating bleeding) or on the bottom (no bleeding) of the aggregate. The comparison of outcome will illustrate to which degree the bleeding effects the stiffness.

The aggregate undergoes an axial compression force and the stress will be calculated, the area being the contact field between aggregate and mortar. The deformation is recorded with LVDTs. The outer gap is created using a *styrofoam* cast, so that the aggregate will have two contact areas with the mortar.

## CONCLUSIONS

Modeling techniques are powerful means for interpretation and explain the ITZ behavior of concrete aggregates. The model will be run with experimentally obtained material properties, and the shear and normal stiffness of the ITZ will be tested based on individual tests.

The FEM as well as mathematical models need to be validated by test results that can represent the actual behavior of the ITZ accurately. The normal and shear ITZ' stiffness will reduce the

iteration since a predicted value is achieved from laboratory test results.

Factors such as surface roughness, bleeding, effect of area can be incorporated in the FEM model. The ITZ area in the model can be approximated by either a single inclusion with a variation in radius, or multiply inclusions with a constant radius.

## REFERENCES

- Abipramono, R., (1997). "*Penambahan Multi Inklusi Baja Terhadap Kekuatan Beton Dalam Tinjauan Dua Dimensi*". Master's Thesis, Institute Teknologi Bandung.
- Akçaoğlu, T., Tokyay, M. and Çelik, T., (2004). "*Effect of Coarse Aggregate Size and Matrix Quality on ITZ and Failure Behavior of Concrete under Uniaxial Compression*", Cement and Concrete Compositions, Vol. 26. pp. 633-638.
- Alexander, K. M., (1959). "*Strength of the Cement-Aggregate Bond*", Journal of the American Concrete Institute, Proc. Vol 56. No. 11, pp. 377-390.
- Barnes, B. D., Diamond, S. and Dolch, W. L., (1978). "*The Contact Zone Between Portland Cement Paste and Glass "Aggregate" Surfaces*", Cement and Concrete Research, Vol. 8. pp. 233-244.
- Barnes, B. D., Diamond, S. and Dolch, W. L., (1979). "*Micromorphology of the Inter-facial Zone Around Aggregates in Portland Cement Mortar*", Journal of The American Ceramic Society, Vol. 62 No. 1-2, pp. 21-24.
- Bentur, A. and Alexander, M. G., (2000). "*A Review of the Work of the RILEM TC 159-ETC: Engineering of the interfacial transition zone in cementitious compositions*", Material and Structures, Vol. 33, March 2000, pp. 82-87.
- Besari, M.S., (2007). "*Review of Some Vital Physical Mechanical Parameters of Concrete*", International Conference on Material

Development in the Concrete Industry, Jakarta, Indonesia.

Bonen, D., (1994). "*Calcium Hydroxide Deposition in the Near Interfacial Zone in Plain Concrete*", Journal of The American Ceramic Society, Vol 77, no. 1 pp 193-196.

Bremner, T. W., and Holm, T. A., (1986). "*Elastic Compatibility and the Behavior of Concrete*", ACI Journal, January-February, pp. 244-250.

Breton, D., Carles-Gibergues, A. and Grandet, J., (1993). "*Contribution to the Formation Mechanism of the Transition Zone Between Rock-Cement Paste*", Cement and Concrete Research, Vol. 23. pp. 335-346.

Christensen, R. M. and Lo, K. H., (1979). "*Solutions for effective shear properties in three phase sphere and cylinder models,*" Journal of Mechanics Physics Solids, Vol. 27, pp.315-330.

Cody, R. D., Cody, A. M., Spry, P. G. and Lee, H., (2001). "*Reduction of Concrete Deterioration by Ettringite Using Crystal Growth Inhibition Techniques*", Iowa DOT TR-431 Report, The Iowa Highway Research Board.

Diamond, D. and Huang, J., (2001). "*The ITZ in Concrete a different view based on SEM observations*", Cement & Concrete Composites, Vol. 23, pp 179-188.

Diamond, S. and Mindess, S., (1991). "*SEM Investigations of Fracture Surface using Stereo Pairs, 1. Fracture Surface of Rock and Cement Paste*", Cement and Concrete Research, Vol. 22 pp. 67-79.

Elsharief, A., Cohen, M. and Olek, J., (2003). "*Influence of Aggregate Type and Gradation on the Microstructure and Durability Properties of Portland Cement Mortar and Concrete*", Cement and Concrete Research, Vol. 33 no. 11. pp. 1837-1849.

Goodier, J. N., (1933). "*Concentration of Stress Around Spherical and Cylindrical Inclusions and Flaws*", Journal of Applied

Mechanics Transactions, ASME, Vol. 55, pp 39-44.

Grassi, P. and Zdeněk, P. B., (2009). "*Random Lattice-Particle Simulation of Statistical Size Effect in Quasi-Brittle Structures Failing at Crack Initiation*" ASCE Journal of Engineering Mechanics, February 2009.

Han, A. L. and Purwanto, (2009). Test Report on Mechanical Properties' of Slag, Pudak Payung and Corresponding Concretes, Construction and Material Laboratory, Diponegoro University, Semarang.

Harutyunyan, V. S., Abovyan, H. S., Monteiro, P. J. M., Vahram P., Mkrtychyan, Balyan, M. K., and Aivazyan, A. P., (2003). "*X-ray Diffraction Investigations of Microstructure of Calcium Hydroxide Crystallites in the Interfacial Transition Zone of Concrete*", Journal of The American Ceramic Society, Vol 86, no. 12 pp 2162-2166.

Hashin Z. and Monteiro, P. J. M., (2002). "*An inverse method to determine the elastic properties of the interphase between the aggregate and the cement paste,*" Cement and Concrete Research, vol. 32, pp 1291-1300.

Head, M.K., Wong, H.S. and Buenfeld, N. R., (2008). "*Characterizing Aggregate Geometry in thin Section of Mortar and Concrete*", Cement and Concrete Research, Vol. 38 pp. 1227-1231.

Kwan, A. K. H., Wang, Z. M. and Chan, H. C., (1998). "*Microscopic Study of concrete II: nonlinear finite element analysis*", Computers and Structures Journal Vol. 70, pp 5454-556.

Mehta, P. K. and Monteiro, P. J. M., (1993). "*Concrete: Microstructures, Properties and Materials*", Third Edition, McGraw-Hill.

Mindess, S., Young, J. F. and Darwin, D., (2003). "*Concrete*", Second Edition, Pearson Education Inc, Upper Saddle River, NJ.

Mitsui, K., Li, Z., Lange, D. A. and Shah, S. P., (1994). "*Relationship between Microstructure and Mechanical Properties of the Pate-*

- Aggregate Interface*", ACI Material Journal Vol. 91, no. 1., pp 30-39.
- Monteiro, P.J.M., Maso, J.C. and Ollivier, J.P., (1985). "*The Aggregate-Mortar Interface*", Cement and Concrete Research, Vol. 15 Nr. 6, pp. 953-958.
- Nagai, K., Sato, Y. and Ueda, T., (2004). "*Mesosopic Simulation of Failure of Mortar and Concrete by 2D RBSM (Rigid Body Spring Model)*", Journal of Advanced Concrete Technology Vol. 2, no 3. pp. 359-374.
- Nagai, K., Sato, Y. and Ueda, T., (2005). "*Mesosopic Simulation of Failure of Mortar and Concrete by 3D RBSM (Rigid Body Spring Model)*", Journal of Advanced Concrete Technology Vol. 3 no. 3. pp. 385-402.
- Neville, A., (1997). "*Aggregate bond and modulus of elasticity of concrete*", ACI Material Journal January-February 1997, pp 71-97.
- Neville, A., (2003). "*Properties of Concrete*", Fourth Edition, Prentice Hall, New Jersey.
- Nie, S and Basaran, C., (2005). "*A Micro-mechanical Model for Effective Elastic Properties of Particulated Composites with Imperfect Interfacial Bonds*", International Journal of Solids and Structures, Vol 42, pp. 4179-4191.
- Nilsen, A. U. and Monteiro, P. J. M., (1993). "*Concrete: A Three Phase Material*", Cement and Concrete Research. Vol. 23 pp. 147-151.
- Pope, A. W. and Jennings, H. M., (1992). "*The Influence of Mixing on the Micro-structure of the Cement Paste/ Aggregate Interfacial Zone and the Strength of Mortar*", Journal of Material Science, Vol. 27. pp. 6452-6462.
- Rao, G.A. and Prasad, B.K.R., (2002). "*Influence of the Roughness of Aggregate Surface on the Interface Bond Strength*", Cement and Concrete Research, Vol. 32 pp. 253-257.
- Rooij, De, M.J. R., Bijen, J. M. J. M. and Frens, G., (1998). "*Introduction to Syneresis in Cement Paste*", Proceedings of the International RILEM Conference 35, E and FN Spon, London, pp. 59-66.
- Roy, D. H., Grutzeck, M. W., Shi, D. and Lui, G., (1993). "*Cement Paste Aggregate Interface Microstructures*", SHRP-C-629, Material Research Laboratory, The Pennsylvania State University.
- Scrivener, K. L. and Pratt, P.L., (1996). "*Characterization of Interfacial Microstructure*", Interfacial Transition Zone in Concrete, RILEM Report 11, London, pp. 3-16.
- Scrivener, K. L., Crumbie, A. L. and Laugesen, P., (2004). "*The Interfacial Transition Zone (ITZ) Between Cement Paste and Aggregate in Concrete*", Interface Science 12, Kluwer Academic Publisher, pp 411-421.
- Sideridis, E., Bourkas, G., Kytopoulos, V., Prassianakis, I. and Younis, C., (2007). "*The Effect of Interface on the Elastic Modulus of Particulate Composites using Two Models of Six and Seven Components*", 4th International Conference on Non Destructive Testing, October 2007, Greece, Athens.
- Šmilauer, V. and Bittnar, Z., (2006). "*Numerical Study of Elastic Properties of ITZ in Hydrating Cement Paste*", 2<sup>nd</sup> International Symposium on Advances in Concrete through Science and Engineering, Quebec, Canada.
- Suarjana, M.; Besari, M.S. and Abipra-mono, R., (1998). "*Two-Dimensional Concrete Models Using Metal Aggregates*", The Interfacial Transition Zone in Cementitious Composites, edd. Katz, A. pp 67-74.
- Vervuurt, A. and Van Mier, J. G. M. (1998). "*Fracture of the Bond between Aggregates and matrix: an Experimental and Numerical Study*", The Interfacial Transition Zone in Cementitious Composites, edd. Katz, A. pp 51-58.
- Zimbelmann, R., (1985). "*A Contribution to the Problem of Cement-Aggregate Bond*", Cement and Concrete Research, Vol. 15. pp. 801-808.

